# AN INVESTIGATION ON THE EFFECTS OF TIME INTEGRATION SCHEMES ON WEAKLY COMPRESSIBLE SPH METHOD

## MARINE 2017

## DENIZ C. KOLUKISA[†], MURAT OZBULUT[*] AND EMRE PESMAN[‡]

[†,‡]Karadeniz Technical University, Faculty of Marine Sciences,
Surmene Deniz Bilimleri Fakultesi, Camburnu, 61530 Trabzon, Turkey
e-mail: [*]dckolukisa@ktu.edu.tr, [‡]pesman@ktu.edu.tr, www.ktu.edu.tr

[*] Piri Reis University, Faculty of Engineering
Piri Reis University Seaside Campus
Postane Mahallesi, Eflatun Sk. No:8, 34940 Istanbul, Turkey
email: mozbulut@pirireis.edu.tr, www.pirireis.edu.tr

**Key words:** SPH Method, Time Integration Schemes, Free Surface Flows, Dam Break Problem

**Abstract.** Temporal discretization is a key aspect of the weakly compressible Smoothed Particle Hydrodynamics (SPH) method, as existing studies prove that the time integration schemes affect the stability of the simulations of weakly compressible SPH [1]. In this study, accuracy and performance of the classical 4th order Runge-Kutta method as a time integration scheme was evaluated by comparing simulation results of 2D dam break problem in terms of pressure and free surface profiles with single step (Euler method), predictor-corrector (midpoint) schemes and existing simulation results given in the literature. Density correction algorithm was utilized as a baseline treatment to prevent density fluctuations. The effect of Artificial Particle Displacement (APD) algorithm is another numerical treatment which is investigated in the present work. It is observed that APD provides more homogeneous particle distribution, leading to a higher accuracy. As for the comparison between time integration schemes, results based on the free surface deformation indicate that the Runge-Kutta method achieves success at reducing the free surface particle scattering encountered on Euler and midpoint schemes.

## 1 INTRODUCTION

Smoothed Particle Hydrodynamics (SPH) method is a meshless numerical method mainly utilized for simulating fluid flow problems. With its fully Lagrangian and meshless nature, the method facilitates simulations of complex geometries and large deformations. Therefore interest of the researchers from ship hydrodynamics studies intensifies with the development and expansion of the method's capabilities.

The SPH method was emerged from astrophysics research by the studies of Gingold and Monaghan [2] and Lucy [3]. Subsequently Monaghan [4] modified the method to simulate free surface fluid flow problems by carrying out dam break, wave maker and beach wave propagation simulations. Monaghan proposed an incompressible fluid approximation by limiting the compressible characteristic of SPH method which was referred to as Weakly

Compressible SPH (WCSPH) approach [4].

In this study, non-viscous Euler equations were implemented, which require an artificial viscosity term in momentum equation to compensate spatial discretization effects [5]. The value of the artificial viscosity term is significant, since it should be determined in conformity with the discretization parameters [6]. In terms of temporal discretization, performance of the classical 4th order Runge-Kutta method as a time integration scheme was compared with implementation of single step Euler method and predictor-corrector midpoint method. The effects of the artificial viscosity were also examined by implementation of four different kinematic viscosity value; $5 \times 10^{-3}$, $1 \times 10^{-3}$, $5 \times 10^{-4}$ and $1 \times 10^{-4}$ [m$^2$/s]. Simulations of 2D dam break problem was run applying three different spatial discretization setup by representing fluid domain with 7200, 11250 and 16200 particles for each time integration scheme and kinematic viscosity combination. Results of the simulations were compared with the experiment results of Pakozdi [7] and SPH simulation results of Ozbulut et al. [8] to present suggestions for future studies. Furthermore an adaptive artificial particle displacement (APD) algorithm along with velocity variance based free surface (VFS) algorithm was implemented.

## 2 NUMERICAL MODELING

### 2.1 Governing Equations

Effects of viscosity can be neglected for the dam break problem. Equation of motion for Newtonian fluids with neglected viscosity is defined by Euler's equation:

$$\frac{d\boldsymbol{u}}{dt} = -\frac{1}{\rho}\nabla p + \boldsymbol{g} \tag{1}$$

$$\boldsymbol{u} = \frac{d\boldsymbol{r}}{dt} \tag{2}$$

where $\boldsymbol{u}$, $\boldsymbol{r}$ and $\boldsymbol{g}$ are velocity, position and gravitational acceleration vectors; $\rho$ and $p$ are density and pressure respectively. The continuity equation is expressed as follows:

$$\frac{1}{\rho}\frac{d\rho}{dt} = -\nabla\boldsymbol{u} \tag{3}$$

In WCSPH method, pressure is determined via implementation of an equation of state for gases. In this study equation of state proposed by Monaghan [6] is utilized:

$$p = \frac{\rho_0 c_0^2}{\gamma}\left[\left(\frac{\rho}{\rho_0}\right)^{\gamma} - 1\right] \tag{4}$$

where $\rho_0$ is reference density and is equal to 1000 [kg/m$^3$] for fresh water, $\gamma$ is the ratio of heat for water and is equal to 7 and $c_0$ is the reference speed of sound. Incompressibility is simulated by enforcing density fluctuations under 1% of the reference density value, which is achieved by restricting Mach number (*M*) under 0.1, thus limiting value of $c_0$ [4, 8, 9]. In this study $c_0$ is taken as 50 [m/s].

## 2.2 SPH Discretization

In SPH, fluid domain is represented by freely moving particles which are treated as interpolation points. As a Lagrangian method, SPH allows these particles to retain their physical identities throughout the simulation period. Value of a function $f$ in a discretized SPH domain is represented with the *kernel approximation*:

$$f(x) = \int f(x')W(x - x', h)\, dx' \tag{5}$$

where $x$ and $x'$ represent coordinate sets of two separate points. $W$ is the kernel function which works as a weighting factor depending directly on the distance between given points limited by the definition of smoothing length "$h$".

Interpolated sum of the neighboring data for an SPH particle is represented with the *particle approximation*. While the neighbor particles of particle $i$ are denoted by $j$, value of the function $f$ and its gradient for particle $i$ in the discretized SPH domain are calculated by following equations:

$$\langle f_i \rangle = \sum_{j=1}^{n} \frac{m_j}{\rho_j} f_j W_{ij} \tag{6}$$

$$\langle \nabla f_i \rangle = \sum_{j=1}^{n} \frac{m_j}{\rho_j} f_j \nabla W_{ij} \tag{7}$$

where $m$ and $\rho$ represents the mass and density of the particles respectively. Various kernel functions are available in literature for utilization of different purposes [10, 11]. In this study quintic spline kernel function was utilized:

$$W(R, h) = \alpha_d \begin{cases} (3-R)^5 - 6(2-R)^5 + 15(1-R)^5, & 0 \le R < 1 \\ (3-R)^5 - 6(2-R)^5, & 1 \le R < 2 \\ (3-R)^5, & 2 \le R < 3 \\ 0, & R \ge 3 \end{cases} \tag{8}$$

where $R = r_{ij}/h$, and $r_{ij}$ is distance of the particle $j$ to the particle $i$ in operating dimension; $\alpha_d$ is a coefficient depending on the dimension of the simulation domain, in this case taken as $7/(478\pi h^2)$ for two dimensions.

Numerical discretization of the governing equations of fluid motion is done by the particle approximation on the Euler's equation and continuity equation, explained with detail in [12]:

$$\frac{d\mathbf{u}_i}{dt} = -\sum_{j=1}^{N} m_j \left( \frac{p_i}{\rho_i^2} + \frac{p_j}{\rho_j^2} + \Pi_{ij} \right). \nabla_i W_{ij} \tag{9}$$

$$\frac{d\rho_i}{dt} = \rho_i \sum_{j=1}^{N} \frac{m_j}{\rho_j} (\mathbf{u}_i - \mathbf{u}_j). \nabla_i W_{ij} \tag{10}$$

where time rate of change of velocity and density of the particle $i$ are calculated directly

without reducing the total derivatives to their local and convective components since we follow the particle according to the Lagrangian description. Artificial viscosity ($\Pi_{ij}$) term in momentum equation (7) is expressed as:

$$\Pi_{ij} = \begin{cases} -\alpha\mu_{ij}\dfrac{c_i + c_j}{\rho_i + \rho_j}, & \boldsymbol{u}_{ij}.\boldsymbol{r}_{ij} < 0 \\ 0, & \boldsymbol{u}_{ij}.\boldsymbol{r}_{ij} \geq 0 \end{cases} \tag{11}$$

$$\mu_{ij} = h\frac{(\boldsymbol{u}_i - \boldsymbol{u}_j).(\boldsymbol{r}_i - \boldsymbol{r}_j)}{\left\|\boldsymbol{r}_i - \boldsymbol{r}_j\right\|^2 + \theta h^2} \tag{12}$$

$$v = \frac{1}{8}\alpha hc \tag{13}$$

where $c_i$ is the local speed of sound for the particle calculated by $c_i = c_0(\rho_i/\rho_0)^{(\gamma-1)/2}$, $\alpha$ is a constant related to kinematic viscosity ($v$) value with respect to the Equation (13) recommended by Monaghan and Kos [6] and $\theta$ is a parameter which has a constant value of 0.05.

## 2.3 Correction Algorithms

*Density correction*: Since the pressure calculation depends on the deviation of density from the reference value by 7th order (see Equation 4), small density disturbances can lead to high oscillations in pressure field. Therefore, a density correction algorithm [8] as a baseline treatment was applied in simulations:

$$\hat{\rho}_i = \rho_i - \sigma\frac{\sum_{j=1}^{N}(\rho_i - \rho_j)W_{ij}}{\sum_{j=1}^{N}W_{ij}} \tag{14}$$

where $\hat{\rho}$ is the corrected density and $\sigma$ is an averaging constant taken as 1 in this work.

*Hybrid VFS+APD algorithm*: Velocity variance based free surface (VFS) and artificial particle displacement (APD) algorithms are corrective tools utilized for preventing particle clustering and noisy pressure. In this study a generalized hybrid formulation was implemented, integrating VFS into APD algorithm covering both free surface and fully populated fluid regions:

$$\sigma\boldsymbol{u}_i = \frac{\sum_{j=1}^{N}(\boldsymbol{u}_i - \boldsymbol{u}_j)W_{ij}}{\sum_{j=1}^{N}W_{ij}} \tag{15}$$

$$\sigma\boldsymbol{r}_i = \sum_{j=1}^{N}\frac{\boldsymbol{r}_{ij}}{r_{ij}^3}r_0^2 u_{cff}W_{ij} \tag{16}$$

$$\hat{\boldsymbol{u}}_i = \boldsymbol{u}_i - \varepsilon\sigma\boldsymbol{u}_i, \qquad \hat{\boldsymbol{r}}_i = \boldsymbol{r}_i - \sigma\boldsymbol{r}_i \tag{17}$$

where $\hat{\boldsymbol{u}}_i$ and $\hat{\boldsymbol{r}}_i$ are the corrected velocity and position vectors, $\varepsilon$ is a constant parameter taken as 0.003, $r_0$ is an averaged sum of neighboring particle distances calculated for each

particle as $r_0 = \sum_j r_{ij}/N$, and $u_{cff}$ is the velocity based APD coefficient linking VFS to APD algorithm calculated by $u_{cff} = |\sigma \boldsymbol{u}_i|$.

## 2.4 Time Integration Schemes

The general form of the time integration schemes utilized in this work is as follows:

$$\beta_i^{n+1} = \beta_i^n + \phi \Delta t \tag{18}$$

While $\beta_i$ represents particle positions, densities or velocities; the function $\phi$ varies with the scheme requiring calculation of the derivatives $d\boldsymbol{u}_i/dt$ and $d\rho_i/dt$ at the beginning point of the iteration"$n$" for *Euler method*, and at the half time step "$(n + 1/2)$" for the modified Euler method also known as the *midpoint method*. The classical fourth order *Runge-Kutta method* has a more sophisticated determination of function $\phi$, assessing and weighting the derivatives calculated once at the beginning, twice at the half step and once at the end of the time step.

## 3 NUMERICAL RESULTS

The 2D dam break problem setup is shown in Figure 1. Dimensions of the problem geometry were set with respect to the experiment setup of Pakozdi [7], defined as $H_w$=0.6 [m], $L_w$=1.2 [m], L=3.23 [m]. Located on the opposite wall $H_p$=0.115 [m] above the ground, pressure measurement point was symbolized with P. Moreover, initial particle pressures for all simulations were set to the Hydrostatic pressure condition.
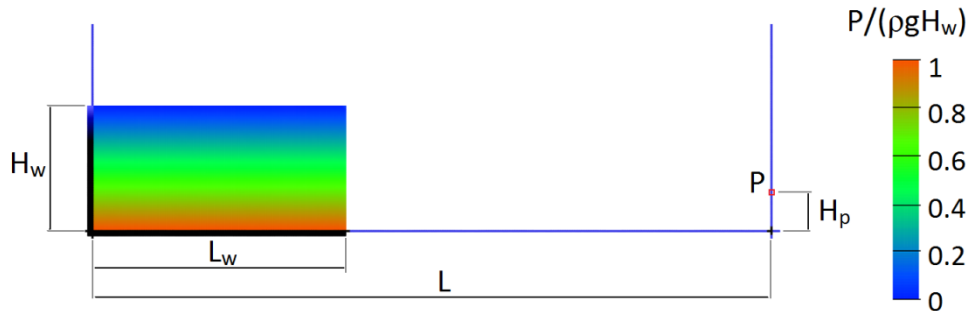


**Figure 1**: Dam break problem setup

Wall boundaries were represented with a single row of solid particles. In order to assure impermeability and for kernel symmetry of the fluid particles near the boundaries, ghost particles were utilized and recreated dynamically at each time step. Particles in the $\Delta r \leq 3h$ neighborhood of solid boundaries were mirrored with respect to the tangent of the wall. Ghost particles have the same mass and density values with the corresponding fluid particles. However the velocity vectors for the particles were mirrored with respect to the free slip condition to reflect the force equilibrium. In addition, the pressure values of the ghost particles below the horizontal wall were adjusted to reflect the hydrostatic pressure difference with respect to the vertical distance. During the simulations, fluid particles with less than 25 neighbor particles were considered as free surface particles and their densities, thereby pressures were set to reference values.

Smoothing length was set fixed as $1.33\Delta x$ for each simulation, where $\Delta x$ represents the initial particle distances in each axis. In terms of spatial discretization, three cases with different initial particle distances were implemented, representing the same fluid domain with 7200, 11250 and 16200 particles. Simulations were run with fixed time steps. Time step sizes were determined with respect to the CFL condition; $\Delta t \leq C_{CFL}\, h_{ij(min)}/c_i + v_{max}$ [8]. The $C_{CFL}$ number was taken as 0.2 for the simulations.

For each time integration scheme and spatial discretization combination, kinematic viscosity values of $5 \times 10^{-3}$, $1 \times 10^{-3}$, $1 \times 10^{-4}$ and $1 \times 10^{-4}$ [m$^2$/s] were employed to assess the effects of artificial viscosity. Kinematic viscosity values were switched via alteration of the variable $\alpha$ (see Equation 11) with respect to the Equation 13. Furthermore hybrid VFS+APD algorithm was applied in extra simulations of $v = 5 \times 10^{-3}$ to represent the effects. Therefore, a 4x3x3 matrix of 36 numerical simulations were created, given in Table 1.

**Table 1**: Simulation matrix; naming of the cases

| Kinematic Viscosity[m$^2$/s] | Number of Particles | Integration Scheme | | |
|---|---|---|---|---|
| | | Euler | Midpoint | Runge-Kutta |
| $5 \times 10^{-3}$ | 7200 | e1 | m1 | rk1 |
| | 11250 | e2 | m2 | rk2 |
| | 16200 | e3 | m3 | rk3 |
| $1 \times 10^{-3}$ | 7200 | e4 | m4 | rk4 |
| | 11250 | e5 | m5 | rk5 |
| | 16200 | e6 | m6 | rk6 |
| $5 \times 10^{-4}$ | 7200 | e7 | m7 | rk7 |
| | 11250 | e8 | m8 | rk8 |
| | 16200 | e9 | m9 | rk9 |
| $1 \times 10^{-4}$ | 7200 | e10 | m10 | rk10 |
| | 11250 | e11 | m11 | rk11 |
| | 16200 | e12 | m12 | rk12 |

Three additional cases were also created utilizing hybrid APD+VFS algorithm on cases m1, m2 and m3. Numerical simulations of the cases were performed by the developed serial C++ code which allows solution of 1 to 14 time steps per second on a single CPU core, depending on the integration scheme and number of particles. In figures 2 to 4; numerical and experimental data of pressure values on the opposite wall at location P were compared in terms of time integration schemes. Results with the same kinematic viscosity values and same number of particles are grouped while only integration schemes vary in each figure.

Figure 2 demonstrate that the viscosity value of $5 \times 10^{-3}$ [m$^2$/s] does not return satisfying results. Besides the delayed arrival of the fluid to the opposite wall, it can be seen that the pressure values fall short of the experimental data. Obviously, lower kinematic viscosity values should return better results since the kinematic viscosity of water is around $1 \times 10^{-6}$ [m$^2$/s]. However as mentioned in earlier sections, discretization is a limiting factor for the viscosity value. Utilization of real viscosity value is inconvenient since it requires extremely small smoothing length, resulting in huge number of particles and infinitesimal time stepping; since decreasing $\alpha$ value itself to a limit without decreasing $h$ value provokes instability
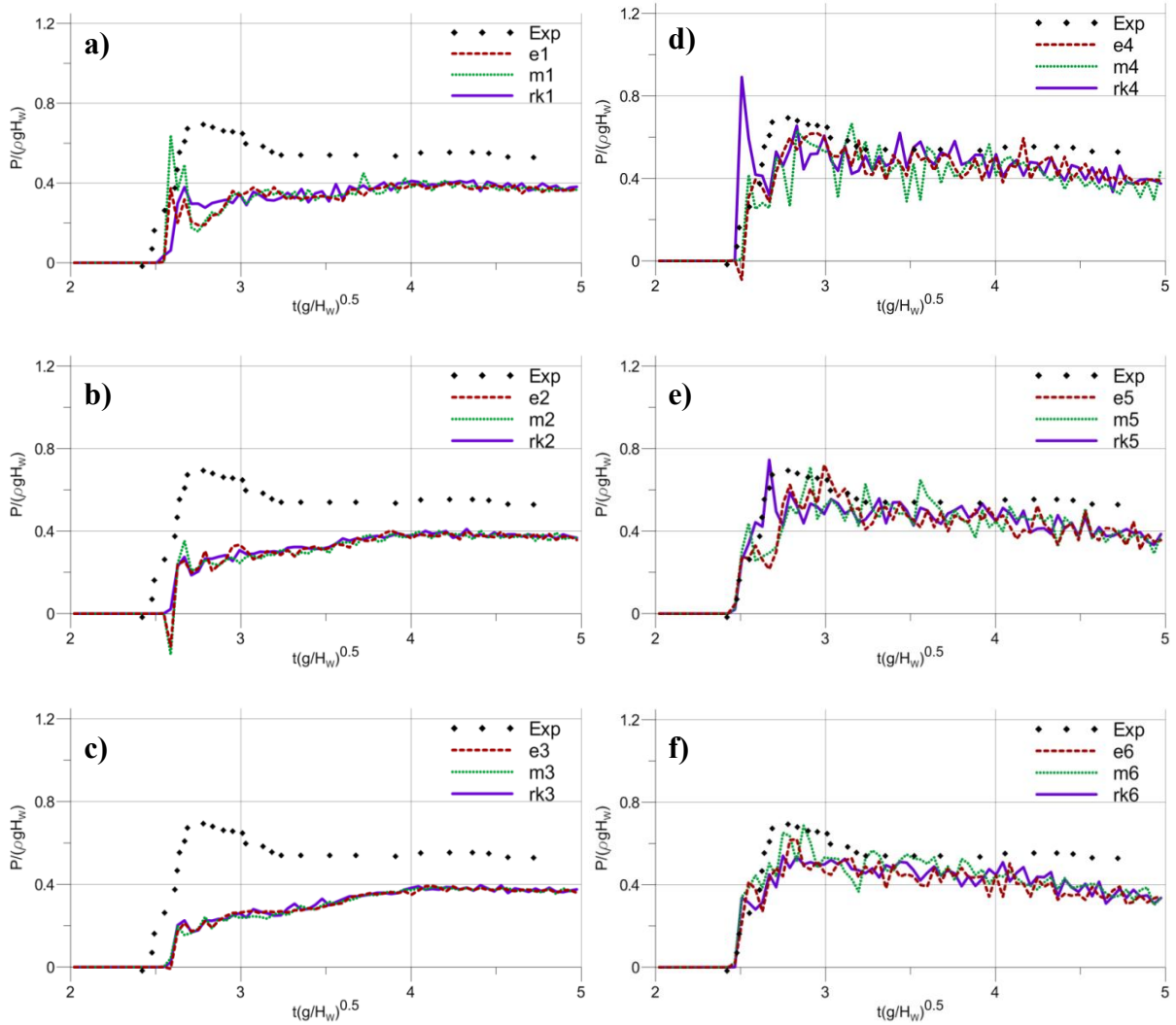
problems causing simulation to collapse.



**Figure 2**: Pressure evaluations; **a)**7200, **b)**11250, **c)**16200 particles for $\upsilon=5\times10^{-3}$ [m²/s]; and **d)**7200, **e)**11250, **f)**16200 particles for $\upsilon=1\times10^{-3}$ [m²/s]

With a decrease of viscosity, numerical results at Figure 2 d, e and f indicate the accurate impact time and adequately matches the pressure levels with a drop in latter stages. However noise of the pressure values are increased comparing to higher viscosity simulations; in contrast, the noise levels are reduced with the increase of the number of particles.

Noise grows larger with the decrease of viscosity in Figure 3 a, b and c. Besides, the noise reduction with the increase of number of particles becomes clearer. Further at Figure 3 d, e and f, noisy characteristic continues however the pressure drop is avoided at the latter stages. It can be claimed that the time integration schemes have a minor effect on the obtained impact pressure results.
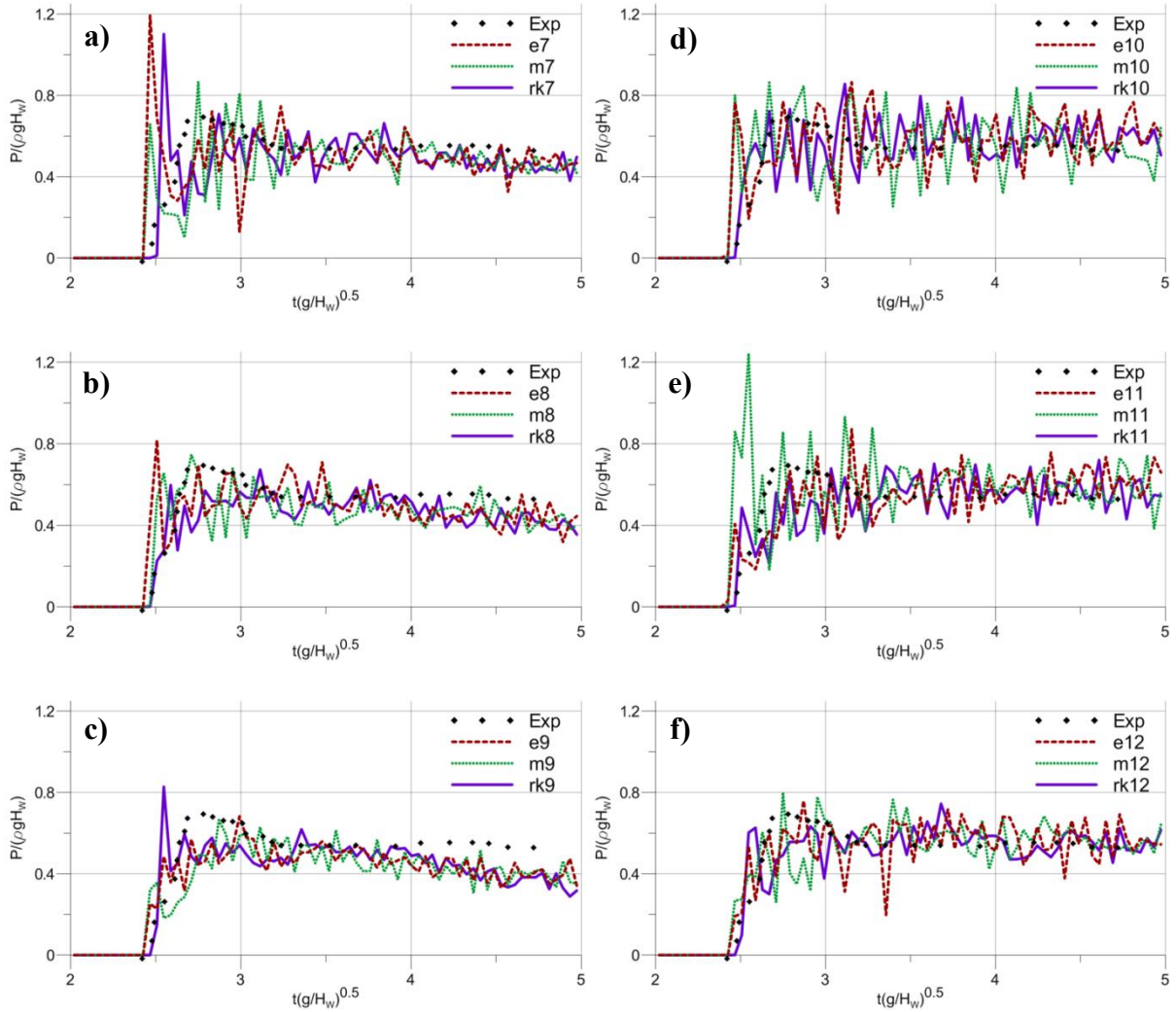
**Figure 3**: Pressure evaluations; **a)**7200, **b)**11250, **c)**16200 particles for $\upsilon=5\times10^{-4}$ [$m^2$/s]; and **d)**7200, **e)**11250, **f)**16200 particles for $\upsilon=1\times10^{-4}$ [$m^2$/s]

As a final remark, it can be inferred from Figure 3 that particle discretization should be finer at lower viscosity simulations to reduce the noise levels of pressure.

To enhance the accuracy of pressure time series for low viscosity simulations, hybrid APD+VFS algorithm is utilized on cases m1, m2 and m3 and results are displayed in Figure 4. Addition of APD and VFS algorithms into the numerical scheme increases the pressure values significantly and yields more compatible results with the experiment data. Nevertheless, the issue of delay due to low viscosity at the arrival on the opposite wall remains unsolved.
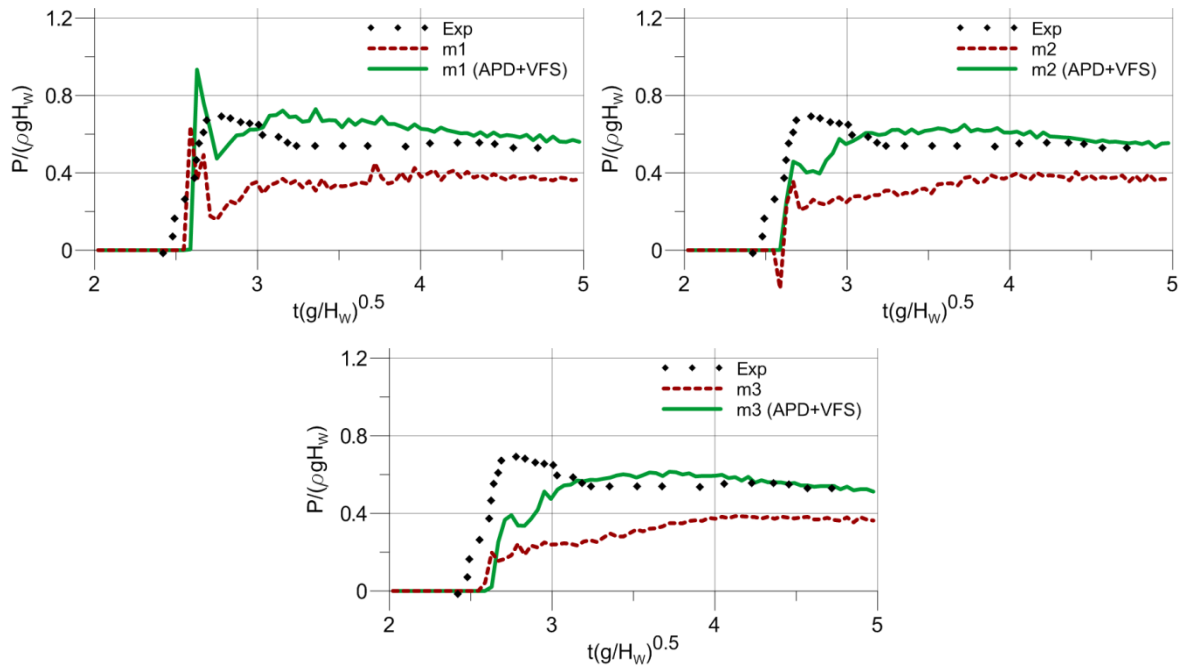
**Figure 4**: Pressure evaluation comparison for m1 with and without APD+VFS

In addition to the pressure results, free surface profiles for m1 with and without APD+VFS algorithms were compared with the existing simulation results of Ozbulut et al. [8] (Fig. 5 and Fig. 6).
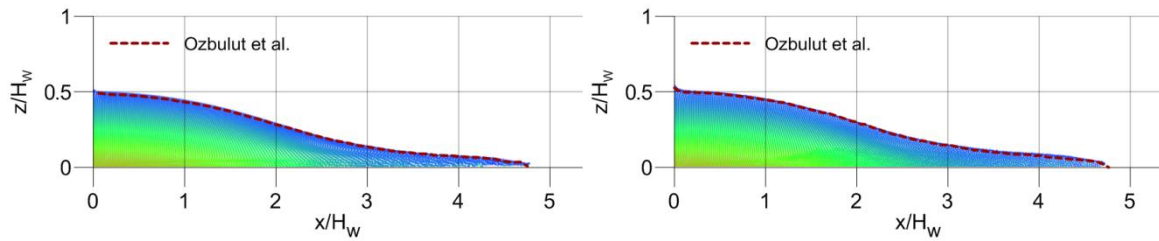


**Figure 5**: Free surface comparisons for simulations for m1 at $t=2.23(H_w/g)^{0.5}$. Left: m1. Right: m1 with APD+VFS
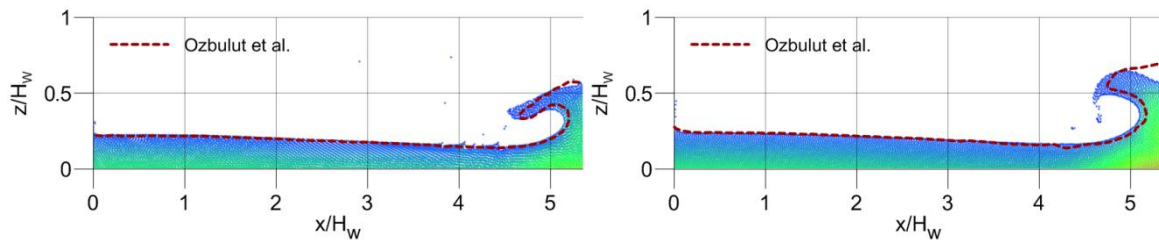


**Figure 6**: Free surface comparisons for simulations for m1 at $t=5.34(H_w/g)^{0.5}$ Left: m1. Right: m1 with APD+VFS

It should be noted that utilization of APD and VFS with a combined fashion is a factor that alters the results which can be seen from right figure at Figure 6. Local determination of the variable $u_{cff}$ in the present study is the main reason behind this difference.
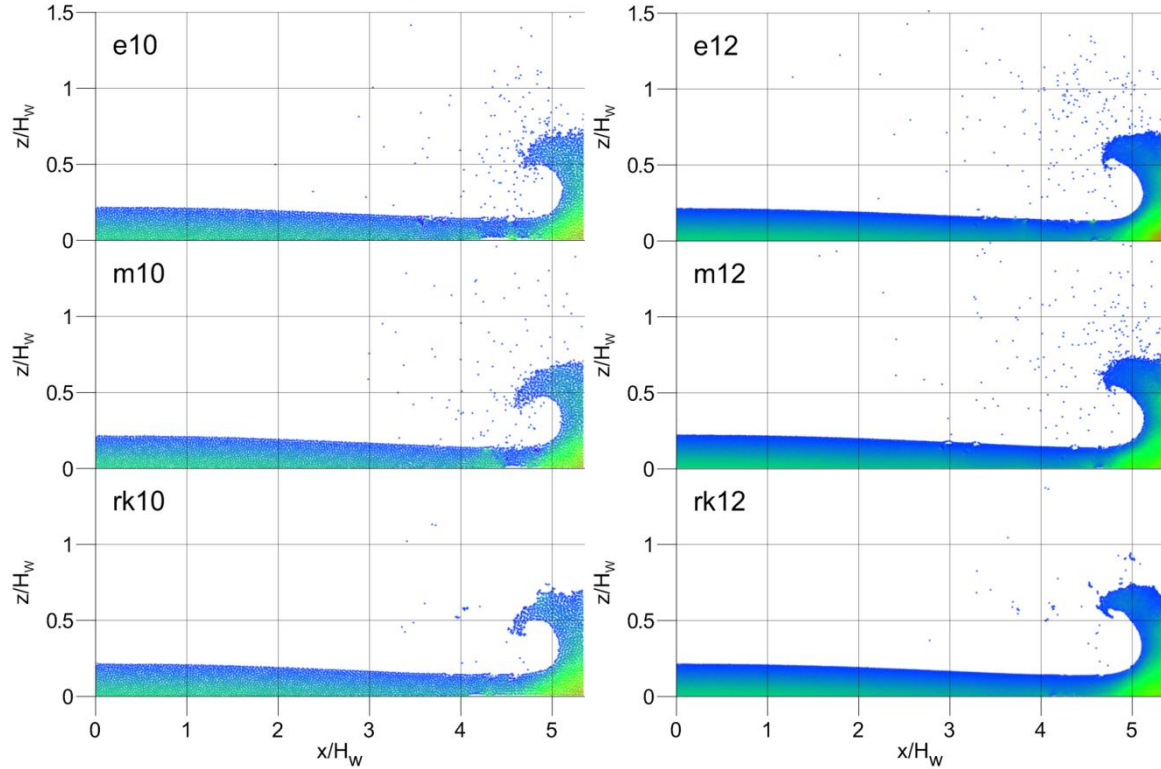


**Figure 7**: Free surface comparisons for simulations for $\upsilon=1\times10^{-4}$ [m$^2$/s] at $t=5.34(H_w/g)^{0.5}$; with 7200 particles (left), with 16200 particles (right).

In Figure 7, effects of the time integration schemes were compared in terms of free surface scattering. Based on the results from Figures 2 and 3, it is seen appropriate to compare the results of simulations with viscosity values of $1\times10^{-4}$ [m$^2$/s], since pressure oscillations are the highest. As it can be seen from Figure 7, Runge-Kutta time integration scheme has a positive effect on reducing the scattered particles due to the impact on the wall.

## 4 CONCLUSIONS

The results of the present work indicate that lower kinematic viscosity produces more accurate, yet oscillatory pressure time series. In contrast, finer discretization reduces the oscillatory characteristics. At the lowest viscosity value ($1\times10^{-4}$ [m$^2$/s]) finer discretization (in this case more than 16200 particles) is required to obtain more satisfying results. On the other hand, at the highest viscosity value ($5\times10^{-3}$ [m$^2$/s]) without APD and VFS algorithm, simulations fail to represent the physical phenomena accurately. In fully populated fluid domain, particle positions are corrected with APD algorithm to prevent particle clustering and disorder. And for the free surface, especially at the impact zone, VFS algorithm helps keeping particles together by velocity correction. Hybrid implementation of both APD and VFS gives

the advantage of having easier adaptation of the code to different physical problem cases by providing local evaluation for velocity and position corrections.

Utilization of different time integration schemes has slight differences on pressure results. Since general pressure characteristics of the WCSPH solution of dam break problem is oscillatory, the nuance can be observed from the free surface forms. The classical fourth order Runge-Kutta method gives the slight edge, however simulation times are about 4 times longer comparing to the Euler time integration method or nearly 3 times longer than the midpoint method. The disadvantage should be compensated by parallel computation possibilities.

## REFERENCES

[1] Violeau, D. and Leroy, A., *On the maximum time step in weakly compressible SPH.* Journal of Computational Physics, 2014. **256**: p. 388-415.

[2] Gingold, R. A. and Monaghan, J. J., *Smoothed Particle Hydrodynamics - Theory and Application to Non-Spherical Stars.* Monthly Notices of the Royal Astronomical Society, 1977. **181**(2): p. 375-389.

[3] Lucy, L. B., *Numerical Approach to Testing of Fission Hypothesis.* Astronomical Journal, 1977. **82**(12): p. 1013-1024.

[4] Monaghan, J. J., *Simulating Free-Surface Flows with Sph.* Journal of Computational Physics, 1994. **110**(2): p. 399-406.

[5] Monaghan, J. J. and Gingold, R. A., *Shock Simulation by the Particle Method Sph.* Journal of Computational Physics, 1983. **52**(2): p. 374-389.

[6] Monaghan, J. J. and Kos, A., *Solitary waves on a Cretan beach.* Journal of Waterway Port Coastal and Ocean Engineering-Asce, 1999. **125**(3): p. 145-154.

[7] Pakozdi, C., *A smoothed particle hydrodynamics study of two-dimensional nonlinear sloshing in rectangular tanks.* 2008, Norwegian University of Science and Technology.

[8] Ozbulut, M., Yildiz, M., and Goren, O., *A numerical investigation into the correction algorithms for SPH method in modeling violent free surface flows.* International Journal of Mechanical Sciences, 2014. **79**: p. 56-65.

[9] Antuono, M., et al., *Free-surface flows solved by means of SPH schemes with numerical diffusive terms.* Computer Physics Communications, 2010. **181**(3): p. 532-549.

[10] Liu, G. R., *Mesh-free methods.. moving beyond the finite element methods.* 2003, Boca Raton: CRC PRESS.

[11] Müller, M., Charypar, D., and Gross, M., *Particle-based fluid simulation for interactive applications*, in *Proceedings of the 2003 ACM SIGGRAPH/Eurographics symposium on Computer animation*, D.L. Breen, M., Editor. 2003, Eurographics Association: San Diego, California. p. 154-159.

[12] Gomez-Gesteira, M., et al., *State-of-the-art of classical SPH for free-surface flows.* Journal of Hydraulic Research, 2010. **48**: p. 6-27.